THE JOURNAL OF BIOLOGICAL CHEMISTRY Vol. 279, No. 31, Issue of July 30, pp. 32018–32027, 2004

Printed in U.S.A.

Preferential Cu^{2+} Coordination by His^{96} and His^{111} Induces β-Sheet Formation in the Unstructured Amyloidogenic Region of the Prion Protein*[S]

Received for publication, March 29, 2004, and in revised form, May 12, 2004
Published, JBC Papers in Press, May 15, 2004, DOI 10.1074/jbc.M403467200

Christopher E. Jones‡§, Salama R. Abdelraheim¶, David R. Brown¶‖, and John H. Viles‡****

From the ¶Department of Biology and Biochemistry, University of Bath, Bath BA2 7AY, United Kingdom and the ‡School of Biological Sciences, Queen Mary, University of London, Mile End Road, London E1 4NS, United Kingdom

The prion protein (PrP) is a Cu^{2+} binding cell surface glycoprotein that can misfold into a β-sheet-rich conformation to cause prion diseases. The majority of copper binding studies have concentrated on the octarepeat region of PrP. However, using a range of spectroscopic techniques, we show that copper binds preferentially to an unstructured region of PrP between residues 90 and 115, outside of the octarepeat domain. Comparison of recombinant PrP with PrP-(91–115) indicates that this prion fragment is a good model for Cu^{2+} binding to the full-length protein. In contrast to previous reports we show that Cu^{2+} binds to this region of PrP with a nanomolar dissociation constant. NMR and EPR spectroscopy indicate a square-planar or square-pyramidal Cu^{2+} coordination utilizing histidine residues. Studies with PrP analogues show that the high affinity site requires both His^{96} and His^{111} as Cu^{2+} ligands, rather than a complex centered on His^{96} as has been previously suggested. Our circular dichroism studies indicate a loss of irregular structure on copper coordination with an increase in β-sheet conformation. It has been shown that this unstructured region, between residues 90 and 120, is vital for prion propagation and different strains of prion disease have been linked with copper binding. The role of Cu^{2+} in prion misfolding and disease must now be re-evaluated in the light of these findings.

Prion diseases are fatal neurodegenerative diseases that include Creutzfeldt-Jacob disease in humans, mad cow disease in cattle, and scrapie in sheep. The infectious agent in transmissible spongiform encephalopathies is a proteinous infectious particle or "prion," which is devoid of nucleic acid. It is believed that these spongiform encephalopathies are caused by the accumulation of an abnormally folded isoform of the cellular prion protein (PrP^C).[1] This misfolded protein is rich in β-sheet and is designated the scrapie isoform, PrP^{Sc} (1–3).

Whereas normal physiological function of the prion protein is yet to be determined, the ability of PrP^C to bind Cu^{2+} *in vivo* and *in vitro* suggests a role in copper homeostasis (4, 5). Indeed, elevated copper levels promote endocytosis of PrP^C suggesting that PrP could transport copper into the cell (6, 7). Recent data has shown that PrP^C expression increased the binding of copper to the outer plasma cell membrane and increases antioxidant enzyme activities (8). Furthermore, it is suggested that PrP^C plays a protective role by binding Cu^{2+} in a redox inactive state (9, 10). An enzymatic role for copper-PrP is also proposed as it exhibits superoxide dismutase activity (11–14).

The cellular prion protein is a cell surface glycoprotein tethered via a glycosylphosphatidylinositol anchor at the C terminus. There are now a number of NMR solution structures of mammalian PrPs in the copper-free form (15–18). A crystal structure of PrP^C has also been published. The structure is dimeric involving domain swapping between monomeric forms (19). Structurally, PrP^C contains two distinct regions. In the absence of Cu^{2+}, the N-terminal domain, residues 23–120, is unstructured (17) and has a high degree of main chain flexibility in the absence of copper (20). In contrast, the C-terminal domain, residues 121–231, is largely α-helical (15). Residues 60–91 consist of an octapeptide sequence, PHGGGWGQ, which is repeated four times. It is this unstructured region that binds four Cu^{2+} ions cooperatively (5). Although binding of a fifth Cu^{2+} ion to PrP has been noted (4, 21, 22), as well as Cu^{2+} coordination to a C-terminal fragment of PrP (23). The majority of studies have concentrated on characterizing the four copper ions binding to the octarepeat region of PrP. Recent publications on copper binding to the octarepeats include circular dichroism (CD) studies (24), electron paramagnetic resonance spectroscopy (EPR) studies (25), and a crystallographic study (26). Dissociation constants for Cu^{2+} binding to the octarepeat region have been reported to be between 1 nM and 10 μM (21, 24) although others have suggested a much higher affinity with a K_d in the femtomolar range (22).

Studies with transgenic mice have shown that mice expressing a truncated version of PrP with the octarepeat region removed are still susceptible to prion infection (27). This has meant that a direct link between copper and prion disease was thought to be unlikely. However, recent studies suggest copper can bind to the unstructured domain of PrP outside of the octarepeat region with a femtomolar dissociation constant (22). Residues His^{111} and/or His^{96} have been implicated in this binding (22, 28, 29). Interestingly, the unstructured region between the N-terminal domain and the structured C-terminal domain is considered to be essential for amyloid formation and infectivity in prion disease (30–33). Residues in this unstructured region are thought to play a pivotal role in the misfolding of

* This work was supported in part by Biochemical and Biophysical Sciences Research Council (BBSRC) Project grants and a University of London Central Research Fund equipment grant. The costs of publication of this article were defrayed in part by the payment of page charges. This article must therefore be hereby marked "*advertisement*" in accordance with 18 U.S.C. Section 1734 solely to indicate this fact.

[S] The on-line version of this article (available at http://www.jbc.org) contains supplemental material.

§ Recipient of a C. J. Martin Postdoctoral Fellowship from the National Health and Medical Research Council, Australia.

‖ Supported by a Senior Fellowship from the BBSRC.

** To whom correspondence should be addressed. Tel.: 44-020-7882-3054; Fax: 44-020-8983-0973; E-mail: j.viles@qmul.ac.uk.

[1] The abbreviations used are: PrP^C, cellular isoform of prion protein; PrP, prion protein; PrP^{Sc}, scrapie isoform of prion protein; TOCSY, total correlation spectroscopy; NOESY, nuclear Overhauser exchange spectroscopy.

PrP^C into the β-sheet-rich conformation (34). The presence of a high affinity Cu^{2+} site within the region 90–126 should have profound implications for the copper loaded structure in this region of PrP^C. Cu^{2+} can convert the cellular prion protein into a protease-resistant species (35). Copper induced structuring in this region might also explain the different protease resistance profiles of PrP observed with and without the presence of Cu^{2+} (36), these protease profiles correspond to similar profiles seen in different strains of prion disease (37). In addition, a fragment from this unstructured region, PrP-(106–126), contains a hydrophobic cluster of residues and has been shown to be neurotoxic in both the soluble and fibrillar states (33, 38). Copper binding to this peptide has been linked with its toxicity (39).

Metal imbalances are a feature of prion disease (40) and metal binding to the prion protein is altered in human prion disease (41). Therefore, it has been suggested that a loss of PrP function in copper transport and homeostasis may well be a feature of prion disease. Recent studies have shown that scrapie infection modulates copper content at a cellular level (42) and that copper-catalyzed redox damage of PrP is implicated in prion disease (43, 44). Elimination of the copper binding octarepeat region has been shown to slow disease progression (27). Additionally, a recent study shows that disease progression in infected mice is slowed with the use of copper specific chelation therapy (45). A mutant form of PrP associated with familial prion disease contains nine additional octarepeats and fails to undergo copper-mediated endocytosis (7). The role of copper in the normal function of PrP, as well as in prion diseases, has been the subject of a number of reviews (46–50).

The aim of this study is to characterize the binding of Cu^{2+} to the unstructured region of PrP outside of the octarepeats. This region is of particular interest because it is essential for amyloidogenesis, and metal occupancy confers strain type in disease. There are some inconsistencies in the literature that we hope to resolve. For example, the coordinating ligands of this so-called fifth Cu^{2+} binding site are disputed with an EPR study, suggesting only His^{96} as the locus for Cu^{2+} coordination (29), whereas an EXAFS study suggested His^{111}, Met^{112}, and His^{96} as coordinating ligands (28). In addition, the reported affinities for Cu^{2+} also vary greatly in the literature between the micromolar (4, 21) and femtomolar (22) dissociation constants. PrP-(23–231) with the octarepeat domain deleted, fragments PrP-(91–115) and PrP-(90–126) and PrP-(91–115) analogues (H96A and H111A) have been used to identify key residues in Cu^{2+} coordination. We use direct spectroscopic methods including CD, NMR, and EPR to study the folding, affinity, coordination geometry, stoichiometry, and pH dependence of copper binding to the prion protein.

EXPERIMENTAL PROCEDURES

Expression and Purification of Recombinant Mouse Prion PrP(23–231Δ51–90) Protein—The coding region of the full-length mouse PrP-(23–231) with a deleted octapeptide region, named PrP(23–231Δ51–90), was cloned into a pET-23 vector to produce a tag-free protein as previously described (11). The protein was expressed in 2-liter flasks of *Escherichia coli* BL21(DE3) cells. Cultures were grown at 37 °C to an A_{600} of 0.7 and the protein expression was induced by the addition of isopropyl-β-D-thiogalactopyranoside to 1 mM. Bacterial pellets were harvested after 3 h and sonicated in a buffer containing 8 M urea, 200 mM NaCl, and 50 mM Tris, pH 7.6. The resulting solution was cleared of bacterial debris by centrifugation at 15,000 rpm for 15 min. The protein was absorbed to a copper-charged metal affinity column made from chelating Sepharose (Amersham Biosciences). The protein was eluted from the column using imidazole (300 mM). The purity of the protein was checked by polyacrylamide electrophoresis and Coomassie staining. The protein was refolded by successive rounds of dilution in distilled water, concentrated using vivaspin concentrator (Vivascience), and dialyzed with a 12,000–14,000 molecular weight cut-off dialysis tube at 4 °C against water overnight to remove residual urea. The concentration of PrP(23–231Δ51–90) was measured by its absorbance at 280 nm ($A^{1\ mg/ml}_{280\ nm}$, 1 cm, = 1.758).

Peptide Synthesis and Purification—Peptides representing various fragments of PrP were synthesized employing solid phase Fmoc (*N*-(9-fluorenyl)methoxycarbonyl) chemistry (A.B.C, Imperial College, London). After removing from the resin and de-protection, the samples were purified using reverse phase high performance liquid chromatography and characterized using mass spectrometry. To mimic the peptides within the full-length prion protein, all peptides were blocked at the N terminus with *N*-acetyl and ethyl ester at the C terminus. One and two-dimensional ^1H NMR spectroscopy confirmed the amino acid sequence.

Design of Peptides—Peptides synthesized included: human (PrP) sequence, PrP-(91–115), acetyl-QGGGTHSQWNKPSKPKTNMKHMAGA; PrP-(90–126), acetyl-GQGGGTHSQWNKPSKPKTNMKHMAGAAAAGAVVGGLG; PrP(H96A), acetyl-QGGGTASQWNKPSKPKTNMKHMAGA; PrP(H111A), acetyl-QGGGTHSQWN KPSKPKTNMKAMAGA; PrP-(58–91), PrP(4octa), acetyl-GQPHGGGWGQPHGGGWGQPHGGGWGQPHGGGWGQ.

Titrations—The pH was measured before and after each spectrum was recorded. Unless otherwise noted, all titrations were carried out in the absence of buffers or salts. For all titrations the pH was adjusted using small aliquots of 100 mM NaOH or HCl. The peptide concentrations were determined using extinction coefficients at 280 nm. An extinction coefficient of 5690 $M^{-1}\ cm^{-1}$ (multiplied by the number of tryptophan residues) was used for each peptide (51). The freeze-dried peptides contained 20–30% moisture by weight. The addition of metal ions ($CuCl_2{\cdot}2H_2O$) or competing ligands was performed using small aliquots from freshly prepared stock aqueous solutions.

Stability Constants—The absolute affinity (pH independent) of L-His for Cu^{2+} is $1.5 \cdot 10^{10}\ M^{-1}$, the apparent affinity, at pH 7.4 is therefore $2.6 \cdot 10^{8}\ M^{-1}$ or a dissociation constant of 3.7 nM (as $\log \alpha = pK_a$, pH = 9.17–7.4 = 1.77, and $\log K_{1(app)} = \log K_1 - \log \alpha = 10.2–1.77 = 8.43$ or $2.6 \cdot 10^{8}\ M^{-1}$). The glycine dissociation constant at pH 7.5 is ~500 nM (52).

Circular Dichroism (CD)—CD spectra were recorded on an AVIV 202 instrument at 25 °C. Typically a cell with a 0.1-cm path length was used for spectra recorded between 185 and 260 nm with sampling points every 0.5 nm. A 1-cm path length cell was used for data between 300 and 800 nm with a 2-nm sampling interval. A minimum of three scans was recorded and the baseline or apospectra were subtracted from each spectrum. Data were smoothed when necessary. Data were processed using Microsoft Excel and the KaleidaGraph spread sheet/graph package. The direct CD measurements (θ, in mdeg) were converted to molar ellipticity, $\Delta\epsilon$ ($M^{-1}\ cm^{-1}$) using the relationship $\Delta\epsilon = \theta/33{,}000 \cdot c \cdot l = [\theta]/3{,}300$, where $[\theta] = \theta/cl$, c is the concentration, and l the path length. The molar ellipticity $[\theta]$ is in units of degree $cm^2\ dmol^{-1}$, therefore, $[\theta] = \{mdeg\}/\{(10) \cdot (mol\ liter^{-1}) \cdot (cm)\}$.

Absorption Spectroscopy (UV-Visible)—UV-visible electronic absorption spectra were obtained with a Hitachi U-3010 double beam spectrophotometer, using a 1-cm path length.

Nuclear Magnetic Resonance (NMR)—All NMR spectra were acquired on a Bruker Advance 600 MHz spectrometer using a 5-mm inverse detection (^1H), triple-resonance, z-gradient probe. Peptide samples were prepared in 90% H_2O, 10% D_2O or 100% D_2O, pH 6.5, or for the Cu^{2+} titrations, pH 7.5, and spectra were acquired at 303 K. In the 90% H_2O, 10% D_2O samples water suppression was achieved using the W5 Watergate method (53), whereas samples in 100% D_2O had residual water suppressed with a low power presaturation pulse. For two-dimensional spectra, quadrature detection in the indirect dimension was achieved using the States-TPPI method. Two-dimensional total correlation spectroscopy (TOCSY) spectra were typically acquired with 2048[F2] × 512[F1] complex points, with water suppression achieved using the W5 Watergate sequence. The TOCSY experiment employed a DIPSI2 sequence for isotropic mixing, with a mixing time of 75 ms (54). Nuclear Overhauser exchange spectroscopy (NOESY) spectra (55) were acquired with 2048[F2] × 512[F1] data points, with mixing times of 200, 300, and 500 ms. Prior to Fourier transformation, sine-squared window functions, phase shifted by 90° were applied to both dimensions, the F1 dimension was forward linear predicted to 512 real points and both dimensions zero filled to 2048 real points. Data were processed using XWINNMR (Bruker) software running on a SGI O_2 work station and analyzed using the program XEASY (56). Proton resonance assignments and sequential connectivities for PrP-(91–115) were obtained using the TOCSY and NOESY data and standard homonuclear techniques (57). Analysis of spectra of the H96A and H111A mutants allowed unambiguous assignment of histidine resonance.

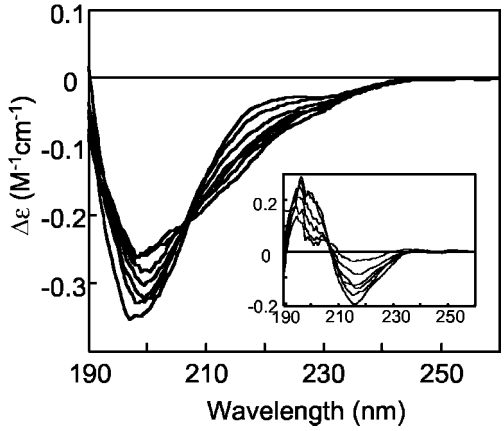

FIG. 1. **Cu^{2+} titration of PrP-(91–115) monitored by CD in the UV region.** 0.085 mM PrP-(91–115), pH 8.4, was titrated with 0.25 mol eq of Cu^{2+}. The spectra show an increase in the negative ellipticity ($\Delta\epsilon$) at 217 nm. The *inset* shows the difference spectra after subtraction of the apo-PrP-(91–115) spectra.

Electron Paramagnetic Resonance (EPR)—X-band EPR spectra were acquired on a Bruker Elexsys E500 spectrometer operating at a microwave frequency of 9.38 GHz. The spectra were acquired over a sweep width of 2500 gauss, a microwave power of 0.63 milliwatt, a modulation frequency of 10 gauss, and a temperature of either 20 or 100 K. At least two scans were acquired per sample. The pH of the peptide samples was adjusted prior to freezing, however, the pH values noted are not altered to take into account freezing effects.

RESULTS

Cu^{2+} Addition Induces β-Sheet Conformation

CD spectra of PrP-(91–115) in the UV region are shown in Fig. 1. In the absence of copper, PrP-(91–115) gives an predominately random coil CD spectrum in agreement with the structure of full-length PrP in this region (17). Fig. 1 shows that addition of Cu^{2+} increases the negative chirality centered at ~217 nm with a decrease in the negative CD band at 200 nm. An isodichroic point is observed at 207 nm with Cu^{2+} addition indicating a single mode of binding up to 1 eq of copper. The changes in the CD spectra with Cu^{2+} additions are more apparent by obtaining the difference spectra shown as an insert. The changes in the CD spectra upon copper coordination indicate an increase in β-sheet or extended conformation, accompanied by a loss of irregular structure. A similar titration with Cu^{2+} and PrP-(90–126), at pH 7.5, produces identical UV-CD spectra (data not shown). Copper binding to His^{111} and His^{96} (14 residues apart) are possible candidates as coordinating ligands and would cause the polypeptide chain to fold back on itself, perhaps inducing anti-parallel β-sheet in this region, the CD spectra shown in Fig. 1 support this possibility. We show later that Cu^{2+} does indeed coordinate to both His^{111} and His^{96}. The Cu-PrP-(91–115) CD data indicates that the copper-loaded peptide still possesses a considerable irregular structure, hence a stable well defined anti-parallel β-sheet between His^{111} and His^{96} is unlikely.

pH Dependence of Cu^{2+} Binding

Using visible absorption bands and associated CD bands we have monitored the pH dependence of Cu^{2+} binding to the prion protein fragment, PrP-(91–115). PrP-(91–115) was loaded with 1 mol eq of Cu^{2+} and the visible absorption spectrum were acquired at a number of pH values between pH 5.5 and 9.4. Fig. 2, *panel A*, shows the resulting overlaid spectra. At pH 5.5, a single absorption band is apparent at 610 nm corresponding to Cu^{2+} d-d electronic transitions. As the pH increases the absorption increases in intensity until ~pH 9. Above pH 6.5 there is a shift in the absorption maximum from 610 to 540 nm, suggesting a

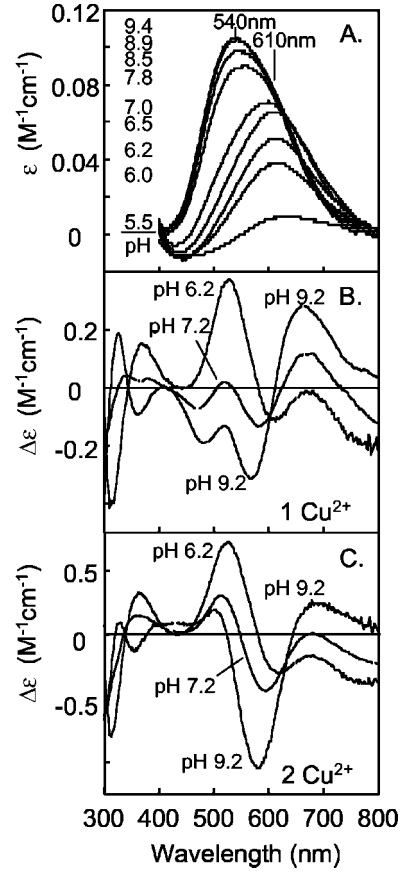

FIG. 2. **pH dependence of Cu^{2+} binding to PrP-(91–115).** *Panel A*, UV-visible spectra of 0.63 mM PrP-(91–115) with 1 mol eq of Cu^{2+} as the pH was incremented from pH 5.5 to 9.4. *Panels B* and *C*, effect of pH on PrP-(91–115) as monitored by CD with 1 and 2 eq of Cu^{2+} added, respectively. Spectra were acquired with ~0.3 mM peptide at pH 6.2, 7.2, and 9.2.

change in the coordination environment of the Cu^{2+} ion. The absorption maximum and extinction coefficient (between 40 and 100 M^{-1} cm^{-1}) for the Cu-PrP-(91–115) complex are typical for a type II Cu^{2+} complex. The absorption maximum can be sensitive to ligand type. For example, using model peptide complexes of type II copper complexes the wavelength maximum decreases from 765 nm for Cu^{2+} with a single nitrogen ligand (and three water oxygens) to 540 nm for Cu^{2+} with four nitrogen ligands (58). The visible absorption spectra observed here are characteristic of three or four nitrogen coordinations in a type II square-planar arrangement.

Circular dichroism spectra of Cu_1PrP-(91–115) (1 mol eq of Cu^{2+} loaded) have been obtained at pH 6.2, 7.2, and 9.2, shown in Fig. 2*B*. These data show that the arrangement of ligands coordinating the Cu^{2+} ions changes significantly with pH. The CD spectrum at pH 6.2 gives a maximum CD band at 520 nm and no ellipticity at 580 nm. In direct contrast, at pH 9.2 a maximal negative CD band at 580 nm is observed with negative ellipticity at 520 nm. The spectrum at pH 7.2 is a mixture of the CD spectra from the mildly acidic and basic conditions. A weighted average of the pH 6.2 and 9.2 spectra shows good agreement with the pH 7.5 spectra using a 70:30% ratio of pH 6.2 and 9.2, respectively. Addition of 2 eq of Cu^{2+} shows further changes in the spectra at all three pH values as shown in Fig. 2*C*.

Copper coordination to PrP-(91–115) is very sensitive to pH. The titratable imidazole side chain of histidine provides a rationale for the pH dependence of binding. The $\Delta\epsilon$ of the d-d transition CD bands indicate a strong vicinal effect from the

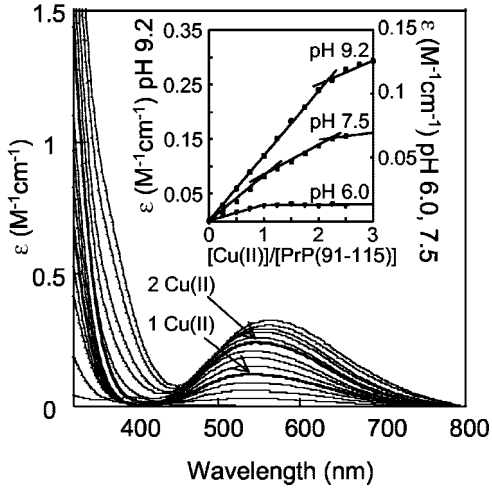

FIG. 3. **Cu^{2+} titration of PrP-(91–115) by UV-visible spectroscopy.** Cu^{2+} was added in 0.25 mol eq relative to PrP-(91–115) (0.32 mM) at pH 9.2. The spectra corresponding to 1 and 2 mol eq of Cu^{2+} are *highlighted*. The *inset* shows the maximum absorption at 550, pH 9.2; 590, pH 7.5; and 610 nm, pH 6.0, as a function of mole equivalents of Cu^{2+}. The *left y* axis shows the absorbance as extinction coefficients for pH 9.2 data, whereas the *right y* axis shows the extinction coefficients for pH 6.0 and 7.5.

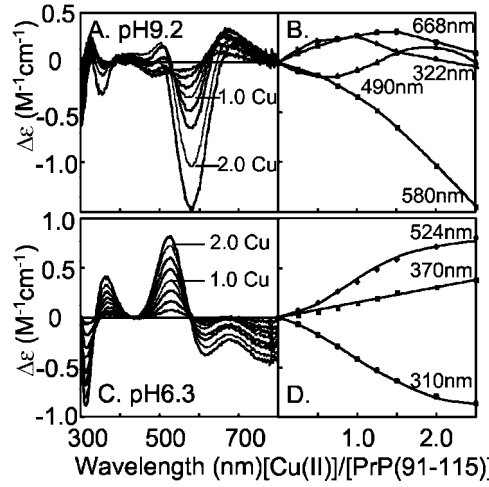

FIG. 4. **CD monitoring of Cu^{2+} binding to PrP-(91–115).** *Panels A* and *C* show 0.25 mol eq additions of Cu^{2+} to PrP-(91–115) at pH 9.2, 0.56 mM; and pH 6.3, 0.70 mM, respectively. The spectra corresponding to 1 and 2 mol eq of Cu^{2+} are *highlighted*. *Panels B* and *D* show the binding curves at various wavelengths plotted as a function of mole equivalents of Cu^{2+} added at pH 9.2 and 6.3, respectively.

chiral Cα, this implies main chain coordination via the carbonyl or amide (59). The change in coordination geometry and ligands as the pH is raised above the pK_a of histidine is likely to be because of the additional coordination of main chain amides as the pH is raised (60).

Cu^{2+} Stoichiometry

To determine the copper binding stoichiometry of PrP-(91–115), increasing amounts of Cu^{2+} were added to each peptide and the visible electronic absorption and accompanying CD bands were monitored. The absorption spectra of Cu^{2+} binding to PrP-(91–115) at pH 9.2 is shown in Fig. 3. The absorption band at 540 nm increases until 2 eq of Cu^{2+} have been added. Beyond 2 eq the spectra display a red shift of the 540 nm peak (to 560 nm at 3 eq) and a significant increase in intensity of the charge transfer band observed below 400 nm.

The Fig. 3, *inset*, shows the mole equivalents of Cu^{2+} added as a function of the absorbance intensity at pH 9.2, 7.5, and 6.0. At pH 7.5 there is a discontinuity in the binding curve at 1 mol eq of Cu^{2+} indicating that the Cu^{2+} ions load onto PrP sequentially. The discontinuity at 1 eq of Cu^{2+} also indicates that there is a significant difference in the affinity between the loading of the first and second Cu^{2+} ion. There is a second discontinuity in the binding curve at 2 eq of Cu^{2+}, this is also observed at pH 9.2 where the absorption peak plateaus at two Cu^{2+} ions. In contrast, at pH 6.2 the absorption saturates soon after 1 mol eq of Cu^{2+} is added.

The titrations described above were also carried out using circular dichroism at pH 6.3 and 9.2 and the CD spectra were acquired between 300 and 800 nm. Fig. 4, *panel A*, shows the pH 9.2 titration, whereas *panel B* shows binding curves at various specific wavelengths. Likewise, the CD spectra at pH 6.3 are shown in Fig. 4, *panel C*, and the accompanying binding curves in *panel D*. The binding curves at pH 9.2 (Fig. 4*B*) show that the CD bands at 322 and 490 nm have abrupt discontinuities after 1 mol eq of Cu^{2+} is added. After 1 eq of Cu^{2+} there is a shift in the isodichroic point at 620 nm. In agreement with the visible absorption spectra at pH 7.5 (Fig. 3, *inset*) it is clear that Cu^{2+} binds to PrP sequentially. Finally, there is a second discontinuity in the 490 nm binding curve at 2 eq of copper, whereas the negative CD band at 580 nm continues to increase in intensity beyond 2 eq of Cu^{2+}, suggesting further weaker Cu^{2+} binding to PrP. At pH 6.2 (Fig. 4, *panel C*) the isodichroic points at 580 and 310 nm remain unchanged between 1 and 2 eq of Cu^{2+}, suggesting that there is a single binding site that saturates only when excess Cu^{2+} is added.

It is clear from the data described in Figs. 3 and 4 that binding of Cu^{2+} to PrP-(91–115) does not complete after 1 or even 2 mol eq additions of copper, as further additions of Cu^{2+} result in further increases in absorbance and CD bands. These bands are not because of free Cu^{2+} ions in solution, as copper free in solution is CD silent and gives a absorption band maximum at ~800 nm, which is not observed. In an attempt to differentiate weak Cu^{2+} binding to PrP-(91–115) from the higher affinity Cu^{2+} binding sites, the prion fragment has been studied (at pH 7.4) in the presence of competing imidazole. Imidazole is a non-chiral molecule and copper-imidazole does not give a CD signal in the visible region (data not shown). In the presence of excess (10 mM) imidazole the CD spectrum of PrP-(91–115) with 4 eq of Cu^{2+}, pH 7.4, looks very similar to the CD spectra of PrP after only 1 eq of copper is added (see Supplementary Materials). This suggests that at pH 7.4 only one copper ion binds to PrP with a significantly higher affinity than imidazole, as even after 4 eq of Cu^{2+} are added in the presence of excess imidazole the spectra appear similar to a single copper bound to PrP-(91–115).

Copper Affinity: Glycine and L-Histidine Competition

The affinity of Cu^{2+} binding to PrP-(91–115) is key to its physiological significance. To investigate the affinity of Cu^{2+} binding to PrP-(91–115) we have used glycine as a copper competitor. Two glycine molecules can bind to one Cu^{2+} with K_a of $1.2 \cdot 10^8$ via both the amino and carboxylate groups (52). The resulting $Cu(Gly)_2$ visible absorption bands are CD silent. Fig. 5, *panel A*, shows the visible region CD spectra for PrP-(91–115) at pH 9.2 as the peptide is titrated to 2 mol eq of Cu^{2+}. A similar competition experiment was also carried out at pH 7.5. The spectra exhibit a number of bands because of d-d electronic absorptions, with major peaks at ~580 and ~688 nm. If glycine was able to successfully compete with PrP-(91–115) for Cu^{2+} ions, then 4 mol eq of glycine would be sufficient to remove both Cu^{2+} ions from the peptide. Fig. 5, *panel A*, clearly shows that even at double the required amount of glycine only a single copper has been abstracted.

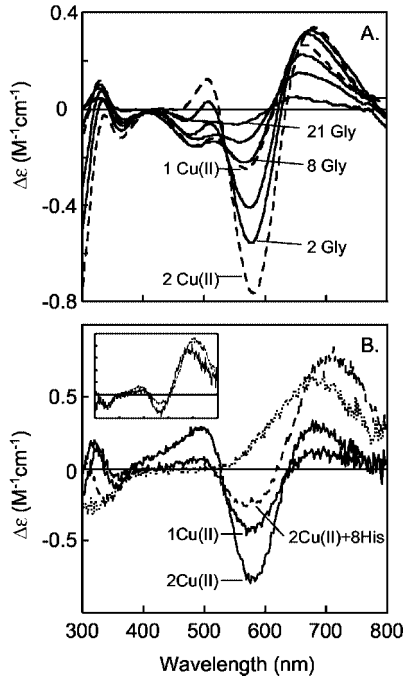

FIG. 5. **Cu^{2+} affinity for PrP-(91–115) from glycine and L-histidine competition, monitored by visible CD.** *Panel A*, Cu_2PrP-(91–115) and glycine competition. *Dashed lines* show 1 and 2 mol eq of Cu^{2+} added to 0.16 mM PrP-(91–115), pH 9.2. The spectra after each addition of glycine are shown with *solid lines*. Spectra corresponding to 2, 8, and 21 mol eq of glycine relative to Cu^{2+} are highlighted. *Panel B*, Cu_2PrP-(91–115) and L-histidine competition. *Solid lines* show 1 and 2 mol eq of Cu^{2+} added to 0.21 mM PrP-(91–115), pH 9.2. The *dashed line* shows the spectra obtained after the addition of 8 mol eq of L-histidine (relative to Cu^{2+}). The *dotted line* shows the spectrum of $Cu(His)_2$. The *inset* shows the spectrum of Cu_2PrP-(91–115) (*dashed line*) in the presence of 4 mol eq of L-histidine compared with a spectrum that is a linear addition of Cu-PrP-(91–115) and $Cu(His)_2$ (*solid line*).

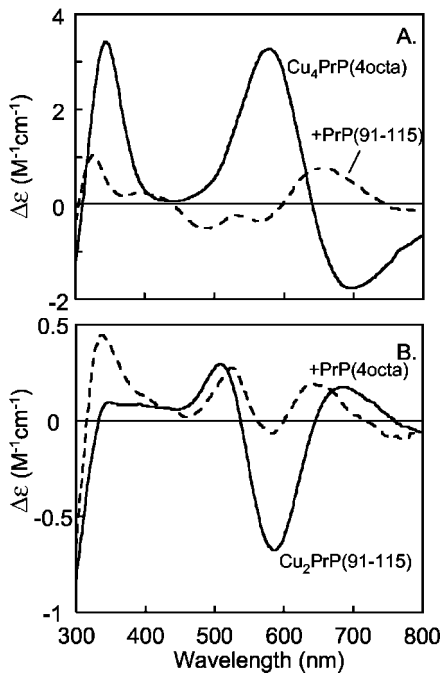

FIG. 6. **CD monitoring of the Cu^{2+} competition between PrP-(91–115) and the octarepeat region, PrP(4octa), pH 7.5.** *Panel A*, *solid line* is 0.05 mM PrP(4octa) fully loaded with 4 mol eq of Cu^{2+}. The *dashed line* shows the spectrum obtained after the addition of 0.2 mM PrP-(91–115). *Panel B*, *solid line* is the spectrum of 0.1 mM PrP-(91–115) loaded with 2 mol eq of Cu^{2+}. The *dashed line* is the spectrum obtained after the addition of 0.05 mM PrP(4octa).

Similarly, at pH 7.5 after 8 mol eq of glycine (relative to peptide) has been added, only a single copper has been abstracted from Cu_2PrP-(91–115). Furthermore, only approximately half of a mole equivalent of copper has been removed from the weaker affinity copper site with 4 eq of glycine. This implies that the low affinity site has a K_a comparable with, but not less than, that of glycine. With 12 mol eq of glycine the CD band at 480 nm gives the same intensity as is observed with 1 mol eq of Cu^{2+}. It appears that the higher affinity site binds to copper at least an order of magnitude higher in affinity than the Cu^{2+}-glycine complex.

In a similar study, free L-histidine was used to compete for Cu^{2+} ions. Fig. 5, *panel B*, shows the effect of adding increasing amounts of L-His to Cu_2PrP-(91–115) at pH 9.2. Histidine has a K_d for Cu^{2+} of 0.1 nM at pH 9.2 and 3 nM at pH 7.4 (52). Unlike $Cu(Gly)_2$, $Cu(His)_2$ is not CD silent and gives a positive CD band at 700 nm, shown in Fig. 5*B*. The weaker binding, second equivalent of Cu^{2+}, is easily removed from PrP causing a reduction in the negative band at 580 nm and an increase in the positive $Cu(His)_2$ CD signal at 700 nm. However, even after twice the required amount of L-His has been added to bind all of the Cu^{2+} present (8 mol eq relative to PrP-(91–115)) the high affinity site remains largely unaffected. This is apparent from the *inset* in Fig. 5, *panel B*. The *inset* compares the CD spectrum of Cu_2PrP-(91–115) in the presence of 4 eq of L-His with a spectrum that is a linear combination of Cu_1PrP-(91–115) and $Cu(His)_2$, the spectra are almost identical. A histidine competition experiment carried out at pH 7.4 has a similar effect. One and 2 mol eq of histidine relative to Cu^{2+} does not significantly perturb the Cu_1PrP-(91–115) CD bands at 480 and 580 nm. Only after 8 mol eq of L-His relative to Cu^{2+} do the CD spectra resemble $Cu(His)_2$.

From these competition studies it is clear that PrP-(91–115) will bind more than 1 eq of Cu^{2+}. The second mole equivalent of Cu^{2+} will bind to PrP with an affinity comparable with glycine, whereas the first, higher affinity binding site will compete successfully for Cu^{2+} in the presence of glycine or even L-His. A single Cu^{2+} ion, at pH 7.4, binds to PrP-(91–115) with an affinity slightly greater than to histidine, indicating a nanomolar dissociation constant for the Cu_1PrP-(91–115) complex.

Competition Studies with PrP(4octa)

There has been much interest in copper binding to the octarepeat region of PrP. We have therefore studied the competitive effect of the octarepeat domain (residues 58–91) on Cu^{2+} binding to the PrP-(91–115) fragment. CD was used, as at pH 7.5 the Cu^{2+} d-d absorption bands of PrP-(91–115) differ significantly from those of Cu_4PrP(4octa) thereby allowing discrimination between copper binding to the two regions of PrP. Fig. 6*A*, shows the effect of the addition of apo-PrP-(91–115) to Cu_4PrP(4octa). The characteristic CD bands at 350, 580, and 680 nm (5, 24) are completely lost with the addition of 1 eq of PrP-(91–115), relative to copper (*i.e.* sufficient PrP-(91–115) to bind the four Cu^{2+} ions bound to the octarepeat in a 1:1 complex). The resulting spectrum is almost identical to the spectrum shown in Fig. 2*B* for Cu_1PrP-(91–115) at pH 7.5. Interestingly, when half the concentration of PrP-(91–115) is used the resultant spectrum does not have the appearance of Cu_2PrP-(91–115). In this situation some of the copper is retained by PrP(4octa). This is more clearly observed when the reverse experiment is performed as shown in Fig. 6*B*. In this case an initial spectrum of Cu_2PrP-(91–115) is obtained and subsequent additions of PrP(4octa) remove some (but not all) of the copper from the lower affinity site of PrP-(91–115). The resulting spectrum in Fig. 6*B* most closely resembles a mixture

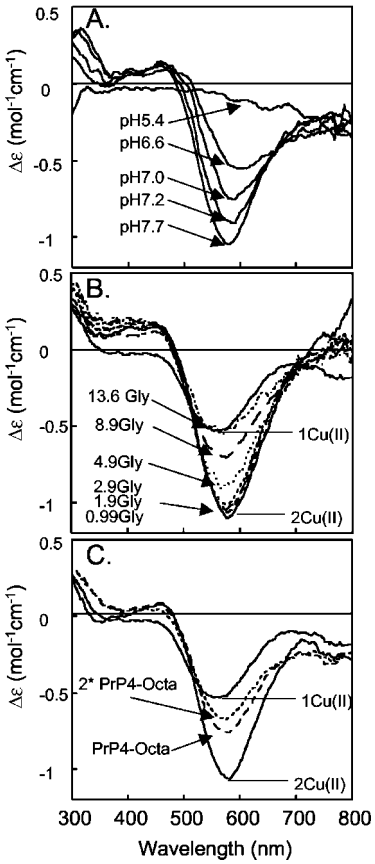

FIG. 7. **CD spectra of Cu_2-PrP(23–231Δ51–90), effect of pH, glycine, and PrP(4octa) competition.** *Panel A*, Cu(II) was added to PrP(23–231Δ51–90) (0.07 mM) to a stoichiometry of ~2 at an initial pH of 5.4 and the resulting CD spectrum acquired over the 300–800 nm range. The pH was incrementally increased and the CD spectrum was obtained at each pH step. *Panel B*, 1 and ~2 (1.8) eq of Cu(II) were added to PrP(23–231Δ51–91) (0.07 mM, pH 7.6) and the CD spectrum was acquired at each addition. Increasing amounts of glycine were added, up to 13.6 mol eq relative to peptide concentration (~8 times Cu(II) concentration) of glycine had been titrated in (*dot-dash lines*). *Panel C*, 1 and 2 eq of Cu(II) were added to PrP(23–231Δ51–91) (0.07 mM, pH 7.5) and the CD spectrum was acquired at each addition. A stoichiometric amount of PrP(4octa) (for Cu(II)) was added to Cu_2-PrP(23–231Δ51–91) and the resultant spectrum was obtained (*dashed line*), then double the stoichiometric amount was added and the CD spectrum was acquired (*dotted line*).

of approximately $Cu_{1.5}$PrP-(91–115) superimposed on a spectrum of $Cu_{1.5}$-PrP(4octa). We have recently shown that glycine will compete for Cu^{2+} ions bound to PrP(4octa) (24). This is in agreement with this study, which shows that two copper ions bind to PrP-(91–115) with a comparable or a greater affinity than glycine. Fig. 6 gives clear evidence that a single Cu^{2+} ion will preferentially bind to PrP-(91–115) rather than the octarepeat region

Cu^{2+} Binding to Full-length PrP Indicates PrP-(91–115) Is a Good Model for Binding to Full-length PrP

So far we have presented pH dependence and glycine competition data for the PrP fragment, residues 91–115. In Fig. 7 we present data for PrP(23–231Δ51–90). Full-length PrP-(23–231) is sparingly soluble at pH 6 and above, however, a construct in which the octarepeats have been removed improves the solubility of the protein between pH 6 and 7.7. This construct contains residues 90–231 necessary for prion propagation with additional N-terminal residues 23–50.

Visible CD spectra shown in Fig. 7 indicate that PrP-(91–115) is a good model for Cu^{2+} binding to full-length PrP. Fig. 7*A* shows

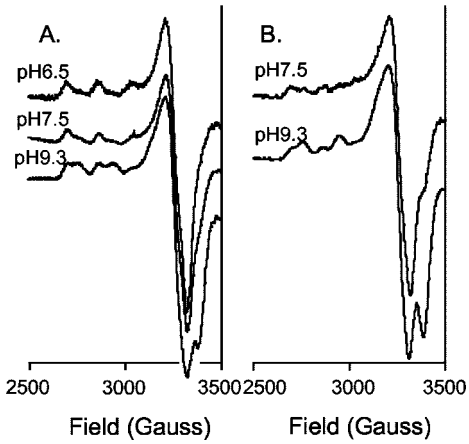

FIG. 8. **EPR spectra of Cu-PrP-(91–115), effect of pH.** *Panel A*, 0.13 mM copper-PrP-(91–115) with 1 mol eq of Cu^{2+} at pH 6.5, 7.5, and 9.3. *Panel B*, 0.13 mM PrP-(91–115) at pH 7.5 and 9.3 with 2 mol eq of Cu^{2+}, spectra were recorded at 20 K.

pH dependence of 2 mol eq of copper binding to PrP(23–231Δ51–90). The visible CD spectra show a close resemblance to Cu_2PrP-(91–115) over the pH range 6.6–7.7. A strong negative band is observed at 600 nm, pH 6.6, which becomes more negative and shifts to 620 nm, pH 7.7. The same band is observed for Cu_2PrP-(91–115) with a similar wavelength and intensity of the CD band. We note there is some variability in the CD bands for Cu_2PrP-(91–115) between 700 and 800 nm, because of baseline instability, but the d-d band at 580–600 nm is very consistent between peptide samples and PrP(23–231Δ51–90).

Fig. 7*B* shows the effect of glycine competition on Cu^{2+} binding to PrP(23–231Δ51–90) at pH 7.6. As with Cu_2PrP-(91–115), glycine can easily abstract the first mole equivalent of Cu^{2+} from Cu_2PrP(23–231Δ51–90). (Note that copper-Gly is CD silent.) Again, as with the PrP-(91–115) fragment, even after the addition of 8 mol eq of glycine, relative to the total amount of Cu^{2+} present, the high affinity Cu^{2+} binding site is unperturbed by glycine.

Finally, in Fig. 7*C* we show, as with PrP-(91–115), the 4octa repeat fragment, PrP-(58–91), does not remove Cu^{2+} from the high affinity Cu^{2+} binding site at pH 7.5. Fig. 7*C* indicates a single Cu^{2+} will preferentially bind to the region between residues 91 and 115, rather than the octarepeats of PrP. The PrP-(91–115) fragment behaves in an identical fashion to PrP(23–231Δ51–90).

It is clear from this data presented in Fig. 7 that the PrP-(91–115) fragment represents a valid model for copper binding to full-length PrP at physiological pH values. Copper-free full-length PrP is unstructured between residues 23 and 126, and as a consequence the small PrP fragment is a good model for Cu^{2+} binding. Visible CD is very sensitive to coordination geometry around the copper ion, however, despite this the spectra of PrP(23–231Δ51–90) show good agreement with Cu_1PrP-(91–115) spectra. In addition, as would be expected, the competition experiments show that the PrP-(91–115) has the same affinity for Cu^{2+} as PrP(23–231Δ51–90).

Coordinating Ligands

EPR—X-band EPR was used to investigate the nature of the groups coordinating the copper ion. EPR spectra of PrP-(91–115) at pH 6.5, 7.5, and 9.3 with 1 and 2 mol eq of Cu^{2+} are shown in Fig. 8, *A* and *B*. In agreement with our optical data the EPR spectra indicate a Type II axial geometry, suggesting a square-planar (tetragonal) arrangement for both 1 and 2 eq of Cu^{2+} at all pH values. Peisach and Blumberg (61) have shown that $A_{\|}$ and $g_{\|}$ values provide details of the nature of the

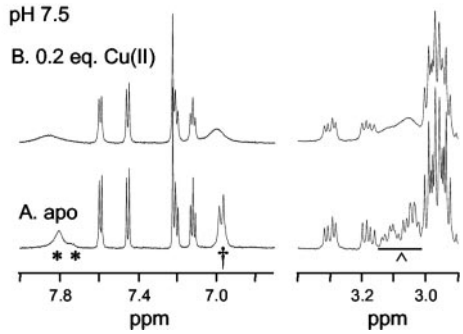

FIG. 9. **^{1}H NMR spectra of PrP-(91–115) at pH 7.5, 0.34 mM.** The spectra are divided into the aromatic (8.0–6.8 ppm), and part of the aliphatic region (3.4–2.8 ppm). The *lower* spectrum (*A*) corresponds to apo-PrP-(91–115), whereas the *upper* spectrum (*B*) corresponds to PrP-(91–115) with 0.2 mol eq of Cu^{2+} titrated in. * highlights the H-ϵ and † highlights the H-δ protons of the histidine imidazole side chain. ^ highlights the signals of the histidine H-β protons.

coordinating atoms. At 1 eq of Cu^{2+} at pH 6.5, a single set of hyperfine splittings are observed with $A_{||}$ and $g_{||}$ values of 15.3 millikaisers and 2.27, respectively. From a Peisach-Blumberg plot (not shown) the EPR spectra are most typical of equatorial coordination of three nitrogen atoms and one oxygen (3N1O) or two nitrogen and two oxygen atoms (2N2O). As the pH is raised a second set of signals are observed. At physiological pH these signals are quite weak, but when the pH is raised to 9.3 the second set of signals have comparable intensity. The $A_{||}$ and $g_{||}$ values observed at higher pH values are 17.0 millikaisers and 2.22. These values fall slightly below the nitrogen/oxygen type II values normally observed implying some distortion in the geometry, but are closest to 3N1O or 4N coordination. Similar behavior to the 1 eq spectra is observed when a second mole equivalent of Cu^{2+} is added, an overlapping set of signals with comparable $A_{||}$ and $g_{||}$ values and similar pH dependence are observed. This supports the visible absorption spectrum that shows a pH dependence shift in maximum from 610 to 540 nm typical of a change from 3N1O to 4N coordination.

Analysis of the EPR data for PrP-(91–115) over a range of pH values shows that the peptide binds copper in a Type II coordination geometry, containing N and O ligands. The EPR spectra presented here for PrP-(91–115) gives $g_{||}$ values of >2.2, which excludes the involvement of sulfur. Based on the observed $A_{||}$ and $g_{||}$ values, the possibility of equatorial coordination via a sulfur ligation from (for example) Met^{112} is unlikely.

Temperature dependence of the EPR spectra was investigated to determine whether there is electron coupling between the Cu^{2+} ions. The overall appearance and line shape of the spectra is relatively unaffected by raising the temperature from 20 to 100 K (data not shown). The lack of temperature dependence in the spectra indicates that histidine bridging between two copper ions, as is seen in Cu_2 superoxide dismutase complex, is unlikely (62).

^{1}H NMR—The effects of Cu^{2+} on the ^{1}H NMR spectrum of PrP-(91–115) peptides were studied to determine the nature of the copper binding site. TOCSY and NOESY were used to fully assign proton resonances in the apo-PrP-(91–115) spectrum at pH values ranging from pH 6.5 to 9.3 (see Supplementary Materials for ^{1}H NMR assignments). Fig. 9 shows that at 0.2 mol eq of Cu^{2+}, pH 7.5, proton resonances corresponding to histidine Hβ, Hϵ-1, and Hδ-2 for both His^{96} and His^{111} are broadened significantly more than other resonances. Furthermore, His^{96} and His^{111} are broadened to an equal extent upon Cu^{2+} addition. The ϵ-CH_3 group of Met^{112} also shows specific broadening.

The electron spin relaxation from the paramagnetic Cu^{2+} resulted in marked broadening of proton NMR resonances linked to the paramagnetic centers by through-bond (contact) or through-space (typically <7 Å) (pseudocontact) interactions. The low levels of Cu^{2+} used (0.2 mol eq) enable the observation of significant differential broadening of the resonances of protons close to the copper binding site. The ^{1}H NMR spectra suggest that the imidazole groups of both His^{111} and His^{96} are involved in coordination of the Cu^{2+}. Based on EPR data the broadening of the ϵCH_3 group of Met^{112} is most likely because of this group being close in space to His^{111} and the paramagnetic ion rather than directly coordinated.

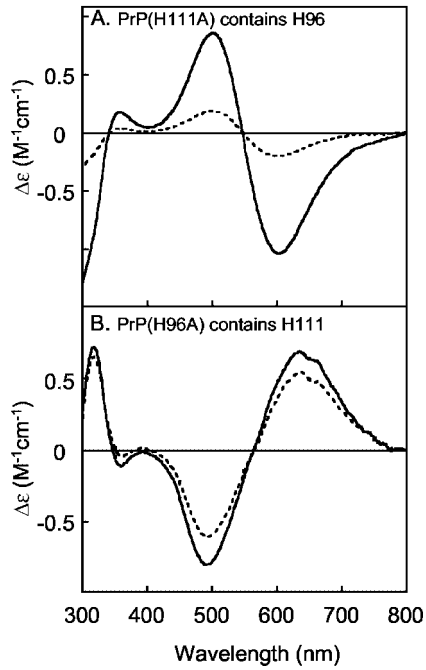

FIG. 10. **Visible CD spectra of copper-PrP analogues PrP(H111A) and PrP(H96A).** *Panel A*, 0.19 mM PrP(H111A), pH 7.6, with 1 mol eq of Cu^{2+} (*solid line*) and the spectrum obtained after the addition of 2 mol eq of glycine (*dashed line*). The decrease in absorption at 600 nm is ~67%. *Panel B*, spectrum of 0.14 mM PrP(H96A), pH 7.7, with 1 mol eq of Cu^{2+} (*solid line*) and the spectrum obtained after the addition of 2 mol eq of glycine (*dashed line*). The decrease in absorption at 500 nm is ~25%.

Analogues PrP(H96A) and PrP(H111A) Indicate a Single Cu^{2+} Ion Coordinates to Both His^{96} and His^{111}

In an attempt to further identify the residues involved in Cu^{2+} binding to PrP-(91–115), two mutants were synthesized with His^{96} and His^{111} replaced with an alanine residue. Fig. 10, *panels A* and *B*, shows the CD spectra in the visible region of PrP(H111A) and PrP(H96A), respectively. Spectra are shown with 1 mol eq of Cu^{2+} added. Both PrP(H96A) and PrP(H111A) give spectra very different from that observed for the wild type fragment after 1 eq of copper, pH 7.6. Weighted combinations of the visible CD spectra for PrP(H96A) and PrP(H111A) also bear no similarity to that PrP-(91–115) spectra. We also note that that position and sign of the visible CD bands for the two analogues are pH independent between pH 7 and 9; unlike the spectra of PrP-(91–115) as shown in Fig. 2, this data is clear evidence that the first, high affinity copper site requires the presence of both His^{96} and His^{111} residues to form a complex.

To gauge the affinity of copper for the two analogues, free glycine was added at pH 7.6. The peptide containing His^{111} only, PrP(H96A), was perturbed by the presence of glycine (with a 25% loss of intensity) as shown in Fig. 10*B*. The peptide containing only His^{96}, PrP(H111A), binds copper even more weakly. A little over half of the copper is removed from

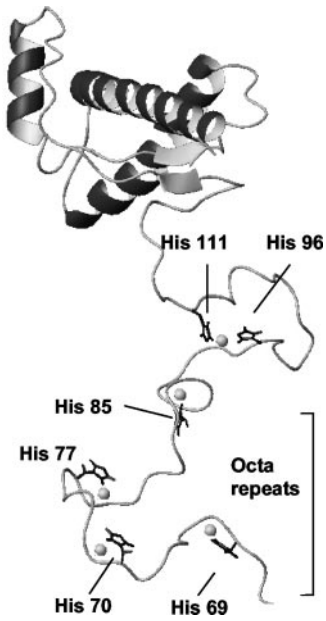

FIG. 11. **Model of PrP-(57–231) showing binding positions of Cu^{2+} ions.** The copper ligating histidine residues are *highlighted* and the copper ions are shown as *spheres*. Distance geometry (Dyana) was used to incorporate a single copper ion at ~2 Å from the N-ϵ atoms of His^{96} and His^{111}. In addition, each HGGGW Cu^{2+} binding motif in the octarepeat region was similarly modeled using the crystal structure as a guide (26). The structured region PrP-(121–231) is from James *et al.* (16). Protein Data Bank accession code is 1B1O.

PrP(H111A) (67%), indicating that Cu^{2+} binds with a comparable affinity to that of glycine. The glycine competition experiments indicate that both PrP(H111A) and PrP(H96A) have an affinity for Cu^{2+} considerably less than PrP-(91–115) (2 to 3 orders of magnitude less) supporting our assertion that Cu^{2+} requires both His^{96} and His^{111} residues to form a complex.

We note that the visible CD spectra for PrP(H96A) and PrP(H111A) are almost mirror images of each other. Visible absorption bands for both analogues are centered at 580 nm with the sign of the CD bands inverted. The hexadecant rule can be used to interpret CD bands in terms of coordination geometry around the metal center (59). The sign of the CD band indicates the position of the side chain relative to the Cu^{2+} coordination plane, and from this it is clear that the position of the ligands are inverted. This possibly reflects amide coordination to the residues N terminus of His^{96} and to the C terminus of His^{111}. The CD of Cu_1PrP(H111A) is almost identical to spectra of a model peptide Cu_1GGGH (N-terminal acetylated) recently reported (63). This supports our assertion that binding of copper to PrP(H111A) is via the imidazole ring of His^{96} and main chain amide nitrogen to the N terminus of His^{96}.

In summary, we have presented compelling evidence that the higher affinity site is a complex that requires both His^{111} and His^{96}. These observations are summarized in Fig. 11.

DISCUSSION

It is now generally accepted that under physiological conditions each of the four histidine-containing octarepeats binds a single Cu^{2+} ion (24, 25). In addition, another copper ion has been suggested to bind to a so-called "fifth site" on PrP (4, 21, 64). His^{96} and/or His^{111} have been implicated in copper coordination (22, 28, 29). We have shown that PrP(23–231Δ51–90) and PrP-(91–115) bind a single Cu^{2+} ion more tightly than the octarepeat region. Competition studies indicate that residues between 91 and 115 can remove copper from the four-octarepeat peptide. A second mole equivalent of copper binds to PrP-(91–115) with a comparable affinity to the octarepeats.

The solubility of full-length PrP at pH values where Cu^{2+} can bind is low, making spectroscopic studies of full-length PrP difficult. A construct in which residues 51–90 have been deleted from PrP-(23–231) has improved solubility. It is clear that between pH 6.6 and 7.7, PrP(23–231Δ51–90) binds to Cu^{2+} in an identical manner to the fragment PrP-(91–115). High affinity Cu^{2+} binding to PrP outside of the octarepeat region explains why it is possible to purify PrP(23–231Δ51–90) using a copper affinity column. We have previously reported Cu^{2+}-bound visible CD spectra for full-length PrP (5). The spectra were obtained with excess Cu^{2+} (25 mol eq) and as a consequence the spectra are dominated by signals from the octarepeats and signals from the high affinity site only were not apparent. EPR studies of copper-bound full-length PrP support the observation that copper binds to the PrP-(91–115) fragment in an identical fashion to the full-length protein (29).

Copper binding in the 91–115 region has been suggested to have a femtomolar affinity (22). Our work suggests a more modest nanomolar dissociation constant, although this is considerably higher than the micromolar dissociation constant suggested by Kramer *et al.* (4, 21). The concentration of extracellular Cu^{2+} is typically 10 μM in blood plasma (65). It is known that a fraction of extracellular Cu^{2+} will bind to L-His in blood plasma (66). From these experiments it is clear that PrP has a higher affinity than L-His for Cu^{2+}. It is therefore initially possible that extracellular PrP will bind Cu^{2+} under physiological conditions. The affinity of PrP for copper supports the *in vivo* studies showing that PrP binds extracellular Cu^{2+} (4).

Based on very strong evidence from our visible CD spectra of PrP(H96A) and PrP(H111A) analogues (Fig. 10), we show that removal of either His^{111} or His^{96} dramatically affects the coordination geometry indicating that both histidines are coordinating ligands to the single high affinity Cu^{2+} site. In contrast, a recent EPR study of PrP-(90–116) suggests that the higher Cu^{2+} affinity site binds only a single histidine (His^{96}) and 3 amide main chain nitrogens to the N terminus of His^{96}. We believe that our data is compelling for both His^{96} and His^{111} binding a single Cu^{2+} ion. If only His^{96} were coordinating the Cu^{2+} ion, as suggested by Burns *et al.* (29), PrP-(91–115) visible CD spectra would have the same appearance at our analogue PrP(H111A), which gives a very characteristic CD spectra for coordination via the imidazole ring and three preceding amide nitrogens. Furthermore, the affinity of Cu^{2+} for PrP(23–231Δ51–90) and PrP-(91–115) for Cu^{2+} are 2 orders of magnitude higher than would be expected for a single imidazole ring and amide main chain coordination. We presume that the EPR study (29) missed this fundamental difference in the complex because after removal of His^{111} a square-planar N/O complex was still formed, although with very different coordination ligands. In this situation, visible CD spectra are much more sensitive to a change in ligands.

In addition to the EPR study of the so-called fifth Cu^{2+} binding site, EXAFS has been used to study copper-PrP-(90–231) (28). EXAFS is a very powerful technique for determining ligand distance from a metal center. However, it is incapable of distinguishing square-planar from tetrahedral coordination and in addition, the scattering difference between N and O ligands is slight. For these reasons, without supporting data, EXAFS can at best only suggest the type of coordination. In addition the EXAFS data were obtained at physiological pH, a pH at which we have shown that more than one coordination species is present. This mixture of species will compromise fitting EXAFS data. Taking on board these caveats, the EXAFS study supports our observations that copper coordinates to both His^{111} and His^{96} (28).

The EXAFS study of PrP-(90–231) (28) suggests nitrogen and oxygen ligands at 1.98 Å. Further out at 3.1 Å, the presence of a sulfur atom improved the EXAFS fit, implicating the involvement of Met^{112} in coordination. Our ^1H NMR data indicates a paramagnetic broadening of the resonance corresponding to the Met^{112} ϵ-CH_3 group on addition of Cu^{2+}. The sulfur atom may be close to the copper center (<7 Å) but any direct coordination to the copper must be an axial, long range interaction, on the basis of our EPR data. Indeed, weakly bound distant ligands axial to the coordination plane generally play only a minor role in magnetic and optical properties of Cu^{2+} complexes (61). We note that His^{96} and His^{111} are conserved in all mammalian species, whereas Met^{112} is not (67). The scattering at 3.1 Å assigned to a Met sulfur ligand is not completely ruled out by our study, but at 3.1 Å from the Cu^{2+} ion it cannot be a key coordinating ligand. Reliable fitting of attenuated EXAFS signal at >3 Å is difficult, in addition the presence of imidazole groups as scatterers will complicate the fitting.

There have also been some spectroscopic studies on Cu(II) binding to the neurotoxic fragment PrP-(106–126) (39, 68). However, the peptide fragment studied did not have its N terminus acetylated, and is therefore not a good model for this unstructured region of the full-length PrP as Cu^{2+} will coordinate to the N-terminal amino group at position 106. Cu^{2+} coordination to the N-terminal amino group of PrP-(106–126) results in very different spectra from acetylated PrP(H96A) used in this study.

It is clear that copper coordination to PrP is very sensitive to pH. Cu^{2+} binding and affinity can be modulated by subtle changes in pH. Cu^{2+} can bind to both the octarepeat region and PrP-(91–115) region at pH values found in the extracellular environment. If the protein is endocytosed via acidified vacuoles, the pH may drop, Cu^{2+} will be released from the octarepeat region but could still be retained by the PrP-(91–115) region at pH 6. The structuring of PrP-(91–115) upon Cu^{2+} binding and subsequent pH-dependent restructuring suggests that the region involving residues 91–115 could play a role in signaling endocytosis of PrP. It has been shown that the octarepeat region is essential for copper-mediated endocytosis (7). Copper binding to the unstructured region outside the octarepeat domain will play a major role in influencing the biological properties of the full-length prion protein. Functionally, this may suggest that the region between the N-terminal octarepeat domain and the structured C-terminal domain acts as a copper-dependent "hinge" region. Copper binding to $His^{96/111}$ could prepare the octarepeat region for copper binding. Indeed, extending the octarepeat region to incorporate residues between 90 and 115 significantly enhances the affinity and cooperatively of Cu^{2+} binding to the octarepeats (21, 64).

Studies that show residues 23–90 are not required for prion propagation (30–32) make the link between disease and Cu^{2+} binding to the octarepeat region unlikely. However, residues 90–120 (unstructured in apo-PrP^C) have been shown to be vital for prion propagation (30–32). Preferential binding of Cu^{2+} to this amyloidogenic region of PrP requires us to re-evaluate the role of copper in prion misfolding and disease. The presence of a high affinity Cu^{2+} site will have profound implications on the copper-loaded structure in this region of PrP^C, and can account for the protease resistance of cellular PrP-(90–231) *in vivo* (36). Intriguingly, Cu^{2+}-dependent protease profiles correspond to similar profiles seen in different strains of prion disease (37). For the first time we have shown that coordination of a single Cu^{2+} ion to both His^{96} and His^{111} has a profound influence on the structuring of this amyloidogenic region inducing a β-sheet like conformation. It is this region of PrP that is thought to be key to prion misfolding and disease, and our data suggests a possible role for Cu^{2+} in triggering this misfolding and amyloidogenesis.

Acknowledgments—We thank Dr. Harold Toms for NMR assistance and NIMR, Mill Hill, for the use of NMR facilities. We also thank Dr. Steve Rigby for assistance with EPR and Prof. Martin Warren for the use of the CD instrument.

REFERENCES

1. Prusiner, S. B. (1997) *Science* **278,** 245–251
2. Horwich, A. L., and Weissman, J. S. (1997) *Cell* **89,** 499–510
3. Prusiner, S. B. (1998) *Proc. Natl. Acad. Sci. U. S. A.* **95,** 13363–13383
4. Brown, D. R., Qin, K., Herms, J. W., Madlung, A., Manson, J., Strome, R., Fraser, P. E., Kruck, T., von Bohlen, A., Schulz-Schaeffer, W., Giese, A., Westaway, D., and Kretzschmar, H. (1997) *Nature* **390,** 684–687
5. Viles, J. H., Cohen, F. E., Prusiner, S. B., Goodin, D. B., Wright, P. E., and Dyson, J. H. (1999) *Proc. Natl. Acad. Sci. U. S. A.* **96,** 2042–2047
6. Pauly, P. C., and Harris, D. A. (1998) *J. Biol. Chem.* **273,** 33107–33110
7. Perera, W. S., and Hooper, N. M. (2001) *Curr. Biol.* **11,** 519–523
8. Rachidi, W., Vilette, D., Guiraud, P., Arlotto, M., Riondel, J., Laude, H., Lehmann, S., and Favier, A. (2003) *J. Biol. Chem.* **278,** 9064–9072
9. Wong, B. S., Pan, T., Liu, T., Li, R., Petersen, R. B., Jones, I. M., Gambetti, P., Brown, D. R., and Sy, M. S. (2000) *Biochem. Biophys. Res. Commun.* **275,** 249–252
10. Shiraishi, N., Ohta, Y., and Nishikimi, M. (2000) *Biochem. Biophys. Res. Commun.* **267**
11. Brown, D. R., Wong, B. S., Hafiz, F., Clive, C., Haswell, S. J., and Jones, I. M. (1999) *Biochem. J.* **344,** 1–5
12. Wong, B. S., Pan, T., Liu, T., Li, R., Gambetti, P., and Sy, M. S. (2000) *Biochem. Biophys. Res. Commun.* **273,** 136–139
13. Brown, D. R., and Besinger, A. (1998) *Biochem. J.* **224,** 423–429
14. Cui, T., Daniels, M., Wong, B. S., Li, R., Sy, M. S., Sassoon, J., and Brown, D. R. (2003) *Eur. J. Biochem.* **270,** 3368–3376
15. Riek, R., Hornemann, S., Wider, G., Billeter, M., Glockshuber, R., and Wuthrich, K. (1996) *Nature* **382,** 180–182
16. James, T. L., Liu, H., Ulyanov, N. B., Farr-Jones, S., Zhang, H., Donne, D. G., Kaneko, K., Groth, D., Mehlhorn, I., Prusiner, S. B., and Cohen, F. E. (1997) *Proc. Natl. Acad. Sci. U. S. A.* **94,** 10086–10091
17. Donne, D. G., Viles, J. H., Groth, D., Mehlhorn, I., James, T. L., Cohen, F. E., Prusiner, S. B., Wright, P. E., and Dyson, J. H. (1997) *Proc. Natl. Acad. Sci. U. S. A.* **94,** 13452–13457
18. Zahn, R., Liu, A., Luhrs, T., Riek, R., von Schroetter, C., Lopez Garcia, F., Billeter, M., Calzolai, L., Wider, G., and Wuthrich, K. (2000) *Proc. Natl. Acad. Sci. U. S. A.* **97,** 145–150
19. Knaus, K. J., Morillas, M., Swietnicki, W., Malone, M., Surewicz, W. K., and Yee, V. C. (2001) *Nat. Struct. Biol.* **8,** 770–774
20. Viles, J. H., Donne, D., Kroon, G., Prusiner, S. B., Cohen, F. E., Dyson, H. J., and Wright, P. E. (2001) *Biochemistry* **40,** 2743–2753
21. Kramer, M. L., Kratzin, H. D., Schmidt, B., Romer, A., Windl, O., Liemann, S., Hornemann, S., and Kretzschmar, H. (2001) *J. Biol. Chem.* **276,** 16711–16719
22. Jackson, G. S., Murray, I., Hosszu, L. L., Gibbs, N., Waltho, J. P., Clarke, A. R., and Collinge, J. (2001) *Proc. Natl. Acad. Sci. U. S. A.* **98,** 8531–8535
23. Brown, D. R., Guantieri, V., Grasso, G., Impellizzeri, G., Pappalardo, G., and Rizzarelli, E. (2004) *J. Inorg. Biochem.* **98,** 133–143
24. Garnett, A. P., and Viles, J. H. (2003) *J. Biol. Chem.* **278,** 6795–6802
25. Aronoff-Spencer, E., Burns, C. S., Avdievich, N. I., Gerfen, G. J., Peisach, J., Antholine, W. E., Ball, H. L., Cohen, F. E., Prusiner, S. B., and Millhauser, G. L. (2000) *Biochemistry* **39,** 13760–13771
26. Burns, C. S., Aronoff-Spencer, E., Dunham, C. M., Lario, P., Avdievich, N. I., Antholine, W. E., Olmstead, M. M., Vrielink, A., Gerfen, G. J., Peisach, J., Scott, W. G., and Millhauser, G. L. (2002) *Biochemistry* **41,** 3991–4001
27. Flechsig, E., Shmerling, D., Hegyi, I., Raeber, A. J., Fischer, M., Cozzio, A., von Mering, C., Aguzzi, A., and Weissmann, C. (2000) *Neuron* **27,** 399–408
28. Hasnain, S. S., Murphy, L. M., Strange, R. W., Grossmann, J. G., Clarke, A. R., Jackson, G. S., and Collinge, J. (2001) *J. Mol. Biol.* **311,** 467–473
29. Burns, C. S., Aronoff-Spencer, E., Legname, G., Prusiner, S. B., Antholine, W. E., Gerfen, G. J., Peisach, J., and Millhauser, G. L. (2003) *Biochemistry* **44,** 6794–6803
30. Muramoto, T., Scott, M., Cohen, F. E., and Prusiner, S. B. (1996) *Proc. Natl. Acad. Sci. U. S. A.* **93,** 15457–15462
31. Fischer, M., Rulicke, T., Raeber, A., Sailer, A., Moser, M., Oesch, B., Brandner, S., Aguzzi, A., and Weissmann, C. (1996) *EMBO J.* **15,** 1255–1264
32. Muramoto, T., DeArmond, S. J., Scott, M., Telling, G. C., Cohen, F. E., and Prusiner, S. B. (1997) *Nat. Med.* **3,** 750–755
33. Brown, D. R., Schmidt, B., and Kretzschmar, H. A. (1996) *Nature* **380,** 345–347
34. Tagliavini, F., Prelli, F., Verga, L., Giaccone, G., Sarma, R., Gorevic, P., Ghetti, B., Passerini, F., Ghibaudi, E., Forloni, G., Salmona, M., Bugiani, O., and Fragione, B. (1993) *Proc. Natl. Acad. Sci. U. S. A.* **90,** 9678–9682
35. Quaglio, E., Chiesa, R., and Harris, D. A. (2001) *J. Biol. Chem.* **276,** 11432–11438
36. Qin, K., Yang, D. S., Yang, Y., Chishti, M. A., Meng, L. J., Kretzschmar, H. A., Yip, C. M., Fraser, P. E., and Westaway, D. (2000) *J. Biol. Chem.* **275,** 19121–19131
37. Wadsworth, J. D., Hill, A. F., Joiner, S., Jackson, G. S., Clarke, A. R., and Collinge, J. (1999) *Nat. Cell Biol.* **1,** 55–59
38. Florio, T., Paludi, D., Villa, V., Principe, D. R., Corsaro, A., Millo, E., Damonte, G., A'rrigo, C., Russo, C., Schettini, G., and Aceto, A. (2003) *J. Neurochem.* **85,** 62–72
39. Jobling, M. F., Huang, X., Stewart, L. R., Barnham, K. J., Curtain, C., Volitakis, I., Perugini, M., White, A. R., Cherny, R. A., Masters, C. L., Barrow, C. J., Collins, S. J., Bush, A. I., and Cappai, R. (2001) *Biochemistry*

40, 8073–8084
40. Thackray, A. M., Knight, R., Haswell, S. J., Bujdoso, R., and Brown, D. R. (2002) *Biochem. J.* **362,** 253–258
41. Wong, B. S., Chen, S. G., Colucci, M., Xie, Z., Pan, T., Liu, T., Li, R., Gambetti, P., Sy, M. S., and Brown, D. R. (2001) *J. Neurochem.* **78,** 1400–1408
42. Rachidi, W., Mange, A., Senator, A., Guiraud, P., Riondel, J., Benboubetra, M., Favier, A., and Lehmann, S. (2003) *J. Biol. Chem.* **278,** 14595–14598
43. Requena, J. R., Groth, D., Legname, G., Stadtman, E. R., Prusiner, S. B., and Levine, R. L. (2001) *Proc. Natl. Acad. Sci. U. S. A.* **98,** 7170–7175
44. Ruiz, F. H., Silva, E., and Inestrosa, N. C. (2000) *Biochem. Biophys. Res. Commun.* **269,** 491–495
45. Sigurdsson, E. M., Brown, D. R., Alim, M. A., Scholtzova, H., Carp, R., Meeker, H. C., Prelli, F., Frangione, B., and Wisniewski, T. (2003) *J. Biol. Chem.* **278,** 46199–46202
46. Brown, D. R. (2001) *Brain Res. Bull.* **55,** 165–173
47. Brown, D. R. (2001) *Trends Neurosci.* **24,** 85–90
48. Lehmann, S. (2002) *Curr. Opin. Chem. Biol.* **6,** 187–192
49. Vassallo, N., and Herms, J. (2003) *J. Neurochem.* **86,** 538–544
50. Millhauser, G. L. (2004) *Acc. Chem. Res.* **37,** 79–85
51. Gill, S. C., and von Hippel, P. H. (1989) *Anal. Biochem.* **182,** 319–326
52. Dawson, R. M. C., Elliot, D. C., Elliot, W. H., and Jones, K. M. (1986) *Data for Biochemical Research*, Claredon, Oxford
53. Liu, M., Mao, X., Ye, C., Huang, H., Nicholson, J. K., and Lindon, J. C. (1998) *J. Magn. Res.* **132,** 125–129
54. Shaka, A. J., Lee, C. J., and Pines, A. (1988) *J. Magn. Res.* **77,** 274–293
55. Jeener, J., Meier, B. H., Bachmann, P., and Ernst, R. R. (1979) *J. Chem. Phys.* **71,** 4546–4553
56. Bartels, C., Xia, T.-H., Billeter, M., Guntert, M., and Wuthrich, K. (1995) *J. Biomol. NMR* **5,** 1–10
57. Wuthrich, K. (1986) *NMR of Proteins and Nucleic Acids*, Wiley, New York
58. Bryce, G. F., and Gurd, F. R. (1966) *J. Biol. Chem.* **241,** 1439–1448
59. Tsangaris, J. M., and Martin, R. B. (1970) *J. Am. Chem. Soc.* **92,** 4255–4260
60. Sigel, H., and Martin, R. (1982) *Chem. Rev.* **82,** 385–426
61. Peisach, J., and Blumberg, W. E. (1974) *Arch. Biochem. Biophys.* **165,** 691–708
62. Valentine, J. S., Pantoliano, M. W., McDonnell, P. J., Burger, A. R., and Lippard, S. J. (1979) *Proc. Natl. Acad. Sci. U. S. A.* **76,** 4245–4249
63. Orfei, M., Alcaro, M. C., Marcon, G., Chelli, M., Ginanneschi, M., Kozlowski, H., Brasun, J., and Messori, L. (2003) *J. Inorg. Biochem.* **97,** 299–307
64. Whittal, R. M., Ball, H. L., Cohen, F. E., Burlingame, A. L., Prusiner, S. B., and Baldwin, M. A. (2000) *Protein Sci.* **9,** 332–343
65. Lentner, C. (ed) (1984) *Geigy Scientific Tables*, Vol. 3, CIBA-GEIGY Ltd., Basel, Switzerland
66. Lau, S., and Sarka, B. (1971) *J. Biol. Chem.* **246,** 5938–5943
67. Wopfner, F., Weidenhofer, G., Schneider, R., von Brunn, A., Gilch, S., Schwarz, T. F., Werner, T., and Schatzl, H. M. (1999) *J. Mol. Biol.* **289,** 1163–1178
68. Belosi, B., Gaggelli, E., Guerrini, R., Kozlowski, H., Luczkowski, M., Mancini, F. M., Remelli, M., Valensin, D., and Valensin, G. (2004) *Chembiochem.* **5,** 349–359

Supplementary material

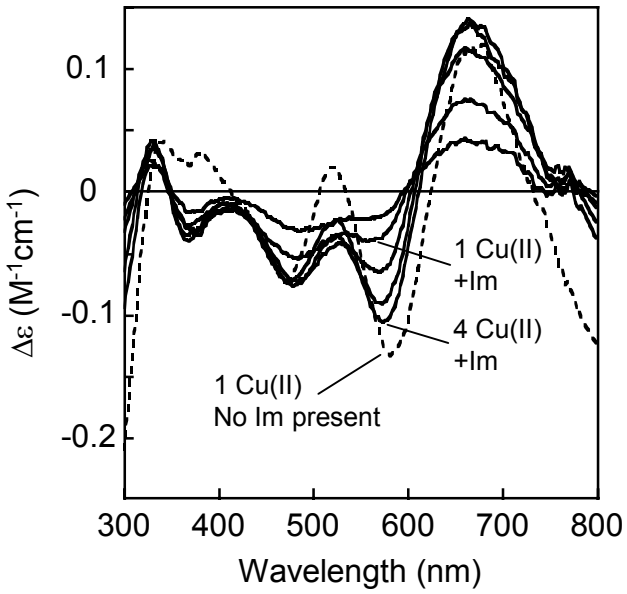

Cu^{2+} titration of PrP(91-115) in the presence of imidazole. 0.23 mM PrP(91-115) pH 7.5, in 10 mM imidazole, was titrated with one, two and four mole equivalents of Cu^{2+}. The *dashed line* shows the spectrum obtained for PrP(91-115) pH 7.2 with one mole equivalent of Cu^{2+} added in the absence of imidazole.

Chemical Shift Data for PrP(91-115)

pH6.5, 303K.

8.346	HN	91	GLN
4.291	HA	91	
2.125	HB2	91	
2.071	HB3	91	
2.352	QG	91	
8.297	HN	94	GLY
3.986	QA	94	
8.067	HN	95	THR
4.267	HA	95	
4.159	HB	95	
1.151	QG	95	
8.539	HN	96	HIS
4.650	HA	96	
3.239	HB2	96	
3.143	HB3	96	
7.228	HD2	96	
8.242	HN	97	SER
4.375	HA	97	
3.781	HB2	97	
3.759	HB3	97	
8.433	HN	98	GLN
4.271	HA	98	
2.154	QG	98	
1.927	HB2	98	
7.369	HE21	98	
6.815	HE22	98	
1.834	HB3	98	
8.074	HN	99	TRP
4.289	HA	99	
3.292	HB2	99	
3.197	HB3	99	
7.229	HD1	99	
7.586	HE3	99	
7.213	HZ3	99	
7.121	HZ2	99	
7.456	HH2	99	
8.093	HN	100	ASP
4.606	HA	100	
2.555	QB	100	
7.963	HN	101	LYS
4.459	HA	101	
1.634	QB	101	
1.375	QG	101	
1.744	QD	101	
4.445	HA	102	PRO
2.296	HB2	102	
2.005	HB3	102	
1.889	QG	102	
3.779	HD2	102	
3.602	HD3	102	
8.375	HN	103	SER
4.417	HA	103	
3.823	QB	103	
8.279	HN	104	LYS
4.611	HA	104	
4.408	HA	105	PRO
2.293	HB2	105	
1.999	HB3	105	
1.890	QG	105	
3.765	HD2	105	
3.601	HD3	105	
8.470	HN	106	LYS
4.331	HA	106	
1.840	HB2	106	
1.757	HB3	106	
1.457	QG	106	
1.704	QD	106	
2.994	QE	106	
8.086	HN	107	THR
4.323	HA	107	
4.165	HB	107	
1.171	QG	107	
8.511	HN	108	ASN
2.812	HB2	108	
2.772	HB3	108	
8.294	HN	109	MET
4.433	HA	109	
2.050	HB2	109	
1.954	HB3	109	
2.560	HG2	109	
2.487	HG3	109	
8.247	HN	110	LYS
4.232	HA	110	
1.718	HB2	110	
1.655	HB3	110	
1.654	HG3	110	
1.374	QG	110	
2.975	QE	110	
8.474	HN	111	HIS
4.329	HA	111	
3.228	HB2	111	
3.155	HB3	111	
7.269	HD2	111	
8.387	HN	112	MET
4.464	HA	112	
1.963	QB	112	
2.558	HG2	112	
2.490	HG3	112	
2.953	QE	112	
8.397	HN	113	ALA
4.316	HA	113	
1.391	QB	113	
8.345	HN	114	GLY
3.932	QA	114	
8.136	HN	115	ALA
4.310	HA	115	
1.377	QB	115	

Preferential Cu^{2+} Coordination by His^{96} and His^{111} Induces β-Sheet Formation in the Unstructured Amyloidogenic Region of the Prion Protein

Christopher E. Jones, Salama R. Abdelraheim, David R. Brown and John H. Viles

J. Biol. Chem. 2004, 279:32018-32027.
doi: 10.1074/jbc.M403467200 originally published online May 15, 2004
